

**This is the preprint version of the contribution published as:**

**Zarejousheghani, M., Schrader, S., Möder, M., Mayer, T., Borsdorf, H. (2018):**  
Negative electrospray ionization ion mobility spectrometry combined with paper-based  
molecular imprinted polymer disks: A novel approach for rapid target screening of trace  
organic compounds in water samples  
*Talanta* **190**, 47 – 54

**The publisher's version is available at:**

<http://dx.doi.org/10.1016/j.talanta.2018.07.076>

# Negative electrospray ionization ion mobility spectrometry combined with paper-based molecular imprinted polymer disks: A novel approach for rapid target screening of trace organic compounds in water samples

Mashaalah Zarejousheghani<sup>a</sup>, Steffi Schrader<sup>b</sup>, Monika Möder<sup>b</sup>, Thomas Mayer<sup>a</sup>, Helko Borsdorf<sup>a\*</sup>

<sup>a</sup> *UFZ – Helmholtz Centre for Environmental Research, Department Monitoring and Exploration Technologies, Permoserstraße 15, D-04318 Leipzig, Germany*

<sup>b</sup> *UFZ – Helmholtz Centre for Environmental Research, Department Analytical Chemistry, Permoserstraße 15, D-04318 Leipzig, Germany*

\*Corresponding author.

E-mail address: helko.borsdorf@ufz.de (H. Borsdorf)

## **Keywords:**

ion mobility spectrometry  
negative electrospray ionization  
water analysis  
artificial sweetener  
Acesulfame K

## **Abstract**

A novel approach for the rapid target screening of water contaminants in trace concentrations was applied for the determination of the artificial sweetener Acesulfame-K, an accepted municipal wastewater indicator. This new method combines the selective enrichment of target analytes on paper-based molecular imprinted polymer disks and the subsequent analysis using a modified ion mobility spectrometer allowing negative electrospray ionization (ESI-IMS). Our developed ion mobility spectrometer permits the sensitive detection of Acesulfame with a limit of detection of 93  $\mu\text{g L}^{-1}$  within few seconds without sample separation. The use of modified paper filters for fast extraction and enrichment of the target substance from water samples results in a lower limit of detection of 0.19  $\mu\text{g L}^{-1}$ . This procedure is directly applicable in the field, the transport and the proper storage of bulky sample bottles is avoided. The capability of the procedure developed was demonstrated by measuring real samples from a river at locations upstream and downstream of the effluent of the central municipal waste water treatment plant. The quantitative data of ion mobility measurements show a very good agreement with those obtained with the commonly used standard procedure (high performance liquid chromatography-tandem mass spectrometry).

## 1. Introduction

Ultra-high performance liquid chromatography (HPLC) coupled to tandem mass spectrometry (MS/MS) or high resolution mass spectrometry (HRMS) with or without enrichment of analytes are state-of-the-art techniques for the determination of trace organic compounds in water samples [1-3]. In spite of their overall performance, these methods are committed to laboratories with proper instrumentation and skilled personnel. Such resources are unavailable for many parts of the world, especially developing countries [4], where a comprehensive water quality monitoring is often necessary due to water scarcity, a limited drinking water supply and restricted possibilities for adequate wastewater treatment [5]. The aim of our work was therefore the development and evaluation of a fast, simple and field deployable analytical approach for the determination of trace organic compounds in water samples.

Only a small number of the available instruments for field analytical chemistry have been proved to allow reliable on-site determination of trace concentrations of emerging contaminants in water [6, 7]. A key advantage of ion mobility spectrometry (IMS) is the ability to perform high speed on-site measurements using handheld or transportable instruments. IMS is operated at atmospheric pressure, the results are available within seconds and different substances can be separated. The separated ions appear as peaks in an ion mobility spectrum in contrast to other sensor techniques which normally provide sum signals [8]. IMS was originally developed for the detection of warfare agents and permits the very sensitive analysis of gaseous compounds.

Electrospray ionization (ESI) for liquid samples is commonly used in HPLC-MS but less applied in IMS. Although the first ESI-IMS couplings were introduced in the eighties, their initial use was limited due to the insufficient desolvation at atmospheric pressure and the resulting low resolution of spectrometers. Different instrumental improvements such as water cooled ESI sources [9, 10] or the incorporation of counter flow heated drift gas [11] were developed. Additionally, the design of the desolvation region in front of the drift tube was optimized, e.g. by reducing of its volume and by adjusting the position of ESI needle [12, 13]. Another approach included the minimization of the solvent amount by attaching nano ESI to IMS [14-16]. However, the application of nanospray emitters goes hand in hand with limited ion transfer into the ion mobility spectrometer and therefore with reduced sensitivities [17]. Nevertheless, these technical modifications led to the availability of functional ESI-IMS couplings, which can be also configured for high-resolution measurements [18, 19]. As there are relatively few examples for negative ESI-IMS in the literature [20], it is therefore important to understand the optimal values of the operational and instrumental parameters.

Advances in miniaturization of IMS hardware will further support the mobility of ESI-IMS for on-site application, for instance, for fast water monitoring. However, ESI-IMS does not tolerate complex matrix compositions which disturb identification and quantification of substances due to the highly complex matrix of the environmental water samples and the resulting matrix effects during the ionization. The coupling with separation techniques as HPLC can overcome these matrix effects. However, such a coupling limits the portability of ion mobility systems and the duration of analysis. Alternatively, an offline sample preparation method can be used to keep the advantages of IMS.

Molecularly imprinted polymers (MIPs) are the cheapest and easiest sorbents to produce of all the available affinity sorbents and they can also tolerate harsh application conditions. MIPs are tailor made polymers where three dimensional cavities containing orientated functional groups are imprinted. These cavities are complementary to the target template molecules [21]. MIPs have been used in various formats as a selective sample preparation technique for the analysis of different matrices including: molecularly imprinted polymer solid phase extraction (MISPE) [22], solid phase microextraction [23], matrix solid-phase dispersion (MSPD) [24] and microextraction by packed sorbent (MEPS) [25]. Swelling and shrinking effects are common features of imprinted polymer sorbents which can be intensified depending on the method used to synthesize the polymers. These effects, along with the reduced size of synthesized polymers, can cause back pressure due to channeling and voiding effects for SPE cartridges filled with these polymer materials. For the selective and fast handling of environmental water samples, a new method was recently developed by our group termed paper-based selective solid phase extraction disk where the MIPs are embedded in filter paper [26]. This method combines different advantages: easy handling without complex equipment, an accelerated sample flow-rate of more than  $30 \text{ mL min}^{-1}$  and the possibility of extracting larger sample-volumes. Back-pressure effects can be reduced due to the geometry of paper-based filters.

Therefore, we developed and evaluated a fast and simple analytical approach integrating the selective enrichment of target analytes on paper-based molecular imprinted polymer disks and their subsequent analysis using ion mobility spectrometry (IMS) equipped with electrospray ionization (ESI). The extraction and enrichment procedure can be performed in the field with very simple equipment and the transportation of water samples is not required.

The capability of this newly developed method is shown with the artificial sweetener Acesulfame-K as target analyte, an accepted municipal wastewater indicator. It passes through the human metabolism comparatively unaffected, is excreted via urine or feces and reaches the sewage system [27]. The reported efficiency with which waste water treatment plants can remove Acesulfame is quite poor (2 – 40 %) [28, 29]. Acesulfame has very good water solubility ( $270 \text{ g L}^{-1}$ ) [30] and its fate

within the aquatic environment is characterized by its persistence in surface waters [31]. It is also comparatively resistant to hydrolysis and biodegradation [32]. It is these properties, its widespread occurrence and its transport in surface and groundwater [33], that make Acesulfame an accepted tracer for sewage flux and provenance [34]. The commonly used analytical instrument for the determination of Acesulfame is LC-MS/MS and several procedures are described in literature [35, 36]. However, Acesulfame has been separated from matrix compounds using ion chromatography [37] and capillary electrophoresis [38] and samples have also been analyzed using different electrochemical methods [39].

## **2. Materials and Methods**

### ***2.1. Production of paper-based molecular imprinted polymer discs***

The procedure for preparing the selective filter paper was adopted from our previous work with modifications [40]. Commercially available laboratory filter papers (19.46 g of Whatman filter paper Grade 3) were simply converted to pulp in water (900 mL) using an ULTRA-TURRAX T-25 dispersing instrument (IKA, Staufen, Germany) at a speed of 9500 min<sup>-1</sup>. 120 mL of the homogenized pulp was diluted again with 900 mL of distilled water to reach a less-dense pulp mixture. This diluted solution was used for the following procedure. A Büchner funnel with a diameter of 47 mm and connection to an adjustable vacuum system was used for fabrication of extraction filters. A commercial cellulose filter (Grade 3) with a thickness of 390 µm (GE Whatman, Dassel, Germany) was positioned at the bottom of the funnel as lower base layer. Using gentle vacuum suction, 30 mL of the paper suspension was added to the filter, which forms a protective layer over the base. The middle composite layer contained 400 mg of ion-exchange imprinted polymer for negatively-charged Acesulfame. The MIPs were synthesized using phase-transfer methodology with (vinylbenzyl)trimethylammonium chloride as the phase transfer reagent, which is a recent development by our group [41]. The polymer was first mixed with 20 mL of MeOH and 40 mL distilled water. This mixture was sonicated to achieve highly dispersed polymer particles. 60 mL of paper suspension were added to this polymer/methanol mixture and thoroughly mixed. The middle composite layer was produced by adding 120 mL of this solution to the Büchner funnel on the top of the lower protective layer. An upper protective layer and commercial filter were added using the same procedure as described for the lower layers. The diameter of our circular disks was adjusted to 47 mm for their use with a manual extraction device which is suitable for field application. The assembled extraction filters were gently pressed, dried by nitrogen gas stream, weighed and stored in a laboratory desiccator for further experiments.

## **2.2. ESI-IMS**

The ion mobility spectrometer used in this study was designed and constructed at the Helmholtz-Centre for Environmental Research. The spectrometer has a traditional stacked ring electrode design with stainless steel ring electrodes of 1 mm thickness and isolators of 5 mm thickness made from Macor. The inner diameter of the electrodes and the isolators within desolvation region (53 mm length) is 10 mm while the drift region has an inner diameter of 20 mm. The drift length between the inlet grid and aperture grid is 113 mm. The aperture grid is positioned a further 1 mm in front of the Faraday plate. Electric fields of  $400 \text{ V cm}^{-1}$  within the desolvation region and of  $410 \text{ V cm}^{-1}$  within the drift region are created by a series of variable and constant resistive voltage dividers. The shutter grid between desolvation region and drift tube was operated with an injection time of  $200 \mu\text{s}$  with a duty cycle of 24 Hz which allows high signal intensities to be measured at an acceptable resolution (sample peaks do not overlap with solvent peaks). A home-made pulse generator in combination with an Agilent 33622A waveform generator (Keysight Technologies, Santa Rosa, USA) was used to apply a pulsed voltage to the shutter grid. Unless otherwise stated, the system temperature remained constant at  $55^\circ\text{C}$  and nitrogen was used as the drift gas with a standard flow rate of  $600 \text{ mL min}^{-1}$ . The ion current at the end of the drift tube was registered by a Faraday plate, amplified using a STEP amplifier (STEP Sensortechnik, Pockau, Germany) and digitized by an Agilent MSO6054A oscilloscope using an averaged signal of 16 measurements (Keysight Technologies, Santa Rosa, USA). All measurements were performed in negative mode.

For ESI, a PicoChip (New Objective, Woburn, USA) equipped a liquid-junction interface and 120 mm uncoated silica tip emitter ( $30 \mu\text{m}$  tip diameter and  $50 \mu\text{m}$  inner diameter of tube) was located approximately 2 mm in front of the first drift ring of the desolvation region which acts as counter electrode for the emitter. This ESI voltage was optimized to 2.3 kV. A commercially available stage (PicoChip for Thermo LTQ) was modified for three-dimensional positioning of the PicoChip and its power supply.

The solvent flow is adjusted using a KDS100 syringe pump (KD Scientific, Holliston, USA) with a  $100 \mu\text{L}$  1710TLLX syringe (Hamilton, Bonaduz, Switzerland). The solvent is transported through PTFE tube with an inner diameter (ID) of 0.45 mm to a three-port valve, which is used for refilling the solvent without opening the system. Via the PTFE tube, the solvent is transported to a 6-port injection valve (A1357, Knauer, Berlin, Germany) where the sample is injected into a  $50 \mu\text{L}$  sample loop. The sample solution is transferred to the PicoChip via a NanoViper tube (Thermo Fisher Scientific, Waltham, USA) with  $50 \mu\text{m}$  ID and a length of 35 cm.

### **2.3. HPLC-tandem mass spectrometry analysis**

HPLC-tandem MS were performed using an HPLC- system "Agilent 1260" (Agilent Technologies, Waldbronn, Germany) coupled with a "QTrap 5500" triple stage quadrupole mass spectrometer (AB Sciex, Darmstadt, Germany). 5  $\mu\text{L}$  of the sample extracts were injected automatically. The chromatographic separation was performed with an "Ascentis Express C18" column (10 cm x 3 mm ID and 2.7  $\mu\text{m}$  particle size, Supelco, Seelze, Germany). Water with 0.1 % acetic acid (solvent A) and methanol with 0.1 % acetic acid (solvent B) were used to separate the target substances at a flow rate of 300  $\mu\text{L min}^{-1}$  and a linear elution gradient started with 95 % solvent A (1 min). Within 15 min the portion of solvent A decreased to 10 % and returned to 95 % between 20 min and 25 min run time. The column oven was set at 30 °C. Electrospray ionization was operated in positive mode at 5.5 kV spray voltage and -4.5 kV in negative ionization mode. Multiple reactions monitoring mode was applied for quantification. Calibration curves with 7 concentration points in tap water were used as the basis for quantification. Instrument blanks were included regularly within each analysis batch.

### **2.4. Sampling and sample preparation procedure**

The selective paper disk was inserted to a filter holder with funnel and base which was connected to a hand-operated vacuum pump with gauge (Sigma-Aldrich, St. Louis, USA). The whole equipment for sampling is shown in Fig. S1 of the supplementary material. In the first step, the paper filter is conditioned with 10 mL of methanol and 10 mL of distilled water for wetting the polymer. The conditioned filter paper was loaded with water sample (commonly 300 mL with a flow rate of 30  $\text{mL min}^{-1}$ ), removed from the filter holder and transferred to a desiccator. The disks loaded in-field can be transported to the laboratory and stored in desiccator at 4°C till further analysis. For elution of analytes, the loaded disk was washed with 10 mL dichloromethane and 10 mL methanol and then eluted with 6 mL methanol/ $\text{NH}_4\text{OH}$  25% (80:20, v/v). The eluate is evaporated to dryness under a gentle air or nitrogen stream and dissolved in 1 mL methanol. In order to reactivate the used selective paper disks for further analysis, 10 mL of methanol and 10 mL methanol/acetic acid (80:20, v/v) were passed through the filter. The reactivated filter-paper was dried using the nitrogen gas stream and stored in a desiccator.

## **3. Results and Discussion**

### **3.1. Adjustment of operational parameters in ESI-IMS**

The ion mobility spectrometer works at atmospheric pressure and a transition from atmospheric pressure to the first vacuum stage is not necessary. The first drift ring normally operates as counter electrode to the ESI needle and as inlet to the desolvation region. Its diameter in conventional ion

mobility spectrometers is between 0.5 and 1 cm. Nearly 100% of the ion plume is therefore transferred into the ion mobility spectrometer [17]. In contrast, most ESI-MS instruments are equipped with pinholes or capillaries with a diameter <500  $\mu\text{m}$  as orifice to MS reducing the transmission of the ion plume. On the other hand, desolvation is not effectively completed before the droplets enter the drift tube [13]. While residues of solvent can be readily evaporated under vacuum conditions of the mass spectrometer, an additional desolvation region is integrated into the ion mobility spectrometer before the ions enter the drift tube.

Based on these considerations, we constructed our ion mobility spectrometer and optimized the design of the inlet and the desolvation region. The optimized configuration is summarized in the experimental part. A 1.0 cm entrance electrode without additional grid inside led to the best ion transmission efficiency and highest signal intensities. By reducing the inner diameter of the desolvation region from 2 cm (drift region) to 1 cm, and therefore increasing the velocity of the preheated gas, complete desolvation of the ions was achieved which lead to stable and reproducible results. The sharp and symmetric peaks in ion mobility spectrum can be seen in Fig. S2 of the supplementary material. The spectra obtained from the same sample on different days showed comparable intensities suggesting a long-term stable response. The optimization of operational parameters was carried out with three substances: Acesulfame, Saccharin and Bentazon. Previous studies indicated a correlation between ESI response in negative mode and  $\log P$ , the logarithm of the octanol-water partition coefficient. The  $\log P$  is used as indicator for analyte polarity and a positive correlation between  $\log P$  and negative ion ESI response was observed [42]. The  $\log P$  values of compounds investigated are -1.06 (Acesulfame), 0.553 (Saccharin) and 1.73 (Bentazon). Other studies found a correlation between negative ESI response and  $\text{pK}_a$ . Compounds with stronger acidity (lower  $\text{pK}_a$  values) tend to higher ionization efficiency [43]. The  $\text{pK}_a$  values are -0.279 (Acesulfame), 1.60 (Saccharin) and 3.28 (Bentazon). All data were taken from [44].

The comparison of different solvents for the determination of small organic molecules with negative ESI indicated that methanol provides higher responses compared to pure water or acetonitrile [42, 45]. Due to the high water solubility of our target analytes, we added increasing amounts of water to methanol. The influence of these solvent compositions is shown in Fig. 1. In contrast to literature, where a general decrease in signal intensities was observed with increasing water content of methanol [46], our results vary depending on the properties of analytes. The addition of water to the methanol causes a clear decrease in response for Acesulfame. The same effect can be observed for Saccharin. However, the decrease in signal intensities is not as significant as detected for Acesulfame. The response of Bentazon is less affected by the water content and the signal intensities are nearly comparable. These results show that the ionization efficiency depends on both the properties of

analytes and the experimental conditions. For further optimization of operational parameters, we used pure methanol as solvent due to the highest signal response for Acesulfame.

The inner diameter and the tip size of spray emitter are important hardware factors for controlling the ESI flow rate. Fig. 2A shows the comparison between two emitters (15  $\mu\text{m}$  tip size and a flow rate of 20  $\mu\text{L h}^{-1}$  vs. 30  $\mu\text{m}$  tip size and a flow rate of 60  $\mu\text{L h}^{-1}$ , the inner diameter was 50  $\mu\text{m}$  for both fused silica emitters). The results clearly confirm the higher sensitivity of Acesulfame signal intensities with increasing ESI flow rate as described above. However, the ESI flow rate can only be varied within a certain range as higher flow rates lead to an instable spray and a peak broadening due to an incomplete desolvation which results in decreasing signal amplitudes (Fig. 2B). The ESI flow rate was optimized to 60  $\mu\text{L h}^{-1}$  for Acesulfame. The temperature of ion mobility spectrometer including desolvation region was adjusted to 55°C according to the results shown in Fig. 2C. The same optimum was found in recent ion mobility measurements in positive mode [19] with ESI operating at atmospheric pressure and methanol as solvent. The microspray ESI needle in our set-up is positioned only few millimeters from the first drift ring, out of which the heated drift gas flows. While higher temperatures lead to improved desolvation, temperatures near the boiling point of methanol (64.8°C) and higher can cause an instable spray with decreasing intensities [10]. The influence of drift gas flow, which also acts as desolvation gas, is shown in Fig. 2D. An increasing gas flow obviously leads to an improved desolvation for Acesulfame and therefore to enhanced signal intensities. As can be generally seen in Fig. 2, all these parameters affect the signal intensity. While Acesulfame and Saccharin generally show a similar dependence of the signal intensity on the experimental conditions, a deviating behavior can be observed for Bentazon which obviously results from its less polar character in comparison to the two other compounds.

In addition to parameters which influence the signal intensity, different experimental conditions can also affect the drift times for the different ions, in particular the temperature of ion mobility spectrometer and the drift gas flow. These results are summarized in Fig. 3. The temperature can generally affect ion mobility in different ways. On the one hand, the temperature has influence on the nature of ions formed, on their degree of clustering and in the case of ESI-IMS on desolvation processes. Therefore, changes in temperature can cause changes in the collisional cross section and the ionic mass which are inversely proportional to ion mobility coefficient. On the other hand, the temperature can influence the drift behavior itself. Due to the combination of these effects, temperature often affects mobility coefficients in a non-linear manner. As can be seen from Fig. 3A, all compounds show negative temperature dependence and have a similar behavior. As the temperature is increased from 25°C to 120°C, the drift time detected reduces by approximately 4 ms

for all substances. This negative, nearly linear temperature dependence indicates that changes in ionic composition or clustering are negligible.

An enhanced drift gas flow causes a slight increase in the pressure inside the drift tube. Therefore, the drift times linearly increase with drift gas flow rate due to the higher gas density and the resulting higher collision frequency between ions and drift gas molecules during the transport through the drift tube. However, these differences are below one millisecond and much less significant in comparison to the influence of temperature. As shown in Fig. 3B, the drift times of all three compounds show a very similar dependence on temperature and drift gas flow. Changes in these parameters have therefore no influence on the peak-to-peak resolution.

### **3.2. Matrix effects using ESI-IMS: Interfering trace organic compounds**

ESI-IMS works without prior separation. The different ions are separated within the drift tube of ion mobility spectrometer within milliseconds after ionization. This principle makes IMS fast and permits measurements in nearly real time. Fig. S2 of the supplementary material shows the obtained ion mobility spectra (in negative mode) of a mixture of Acesulfame-K, Bentazon, Saccharin, Ibuprofen sodium salt, Naproxen sodium salt, Atrazine and Caffeine (where the concentration of each solute was  $10 \text{ ng } \mu\text{L}^{-1}$ ). The spectrum shows three sharp and fully separated peaks for Acesulfame-K, Bentazon and Saccharin. Ibuprofen (18.04 ms) and Naproxen (18.45 ms) can also be detected. However, the product ion peaks of both substances are not completely separated. Atrazine and Caffeine do not provide a signal in negative mode. Although our target analyte can be clearly separated from interfering compounds, it is necessary to evaluate their influence on quantification.

Other trace organic compounds occurring in the water samples can also co-elute with Acesulfame from the paper filter. MIPs do not have a selectivity of 100% and especially substances with structural similarities can be co-eluted. These components can cause ionization suppression that negatively affects the quantification. This ion suppression is related to changes in liquid-to-gas transfer efficiency or charge transfer efficiency of competing ions. Both effects with a possible influence on quantitative results were investigated. For this purpose, we investigated the signal intensity of Acesulfame in dependence on the occurrence of different additional trace organic compounds (Acesulfame, Saccharin, Bentazon, Ibuprofen, Naproxen, Caffeine and Atrazine). The selected compounds are typical ubiquitously occurring substances which are widely spread in natural waters. The results are summarized in Fig. 4. The graphs in Fig. 4A show the signal intensity of Acesulfame as individual compound and in the presence of additional matrix compounds with the same concentration as labeled on the abscissa. Especially Saccharin and Bentazon have a considerable influence on the peak intensity of Acesulfame. The signal intensity of Acesulfame

decreases to 80% in the presence of Saccharin and to approximately 50% in the presence of Bentazon related to pure Acesulfame. A mixture of Saccharin and Bentazon reduces the signal intensity in a similar way as observed for Bentazon alone. A comparable effect can also be observed for a mixture of all seven compounds where the sensitivity of the detector towards Acesulfame is reduced to 50%. The most significant influence on the signal intensity of Acesulfame can therefore be observed for Bentazon.

Due to the comparative high concentrations used in this experiment, we evaluated the influence of Bentazon on the signal intensity of Acesulfame within lower concentration ranges. Different methanol solutions containing Acesulfame and Bentazon were prepared and analyzed. The concentration of Acesulfame was kept constant ( $5 \text{ ng } \mu\text{L}^{-1}$ ) and the concentration of Bentazon was increased from 0 to  $4.97 \text{ ng } \mu\text{L}^{-1}$ . The obtained results (Fig. 4B) show that the presence of Bentazon reduces the signal intensity of Acesulfame in the same way as observed above. A concentration ratio of 1:1 ( $5 \text{ ng } \mu\text{L}^{-1}$  for each compound) leads also to a reduction of the signal intensity of Acesulfame to 50%. For this reason, the selective separation of Acesulfame from the sample matrix before the analysis using ESI-IMS has a particular importance.

### ***3.3. Matrix effects using ESI-IMS: Dissolved organic matter***

In addition to other trace organic compounds, natural aquatic systems also contain dissolved organic matter (DOM), a fraction of a broad variety of soluble organic materials with very different physicochemical properties. The DOM content of natural waters is typically in the range up to  $10 \text{ mg L}^{-1}$ . DOM can influence the sample preparation due to the presence of an interfering matrix. Parts of these organic materials can also be transferred to the eluate if they are not completely separated by our sample preparation procedure.

Fig. 5 shows the influence of DOM on the ESI measurement without sample preparation. For this purpose, soluble humic acid sodium salt was dissolved in methanol in concentrations up to  $100 \text{ ng } \mu\text{L}^{-1}$ . Furthermore, a constant concentration of Acesulfame ( $0.975 \text{ ng } \mu\text{L}^{-1}$ ) was added to each methanolic DOM sample. This solution was directly injected to the ESI source of the IMS. Although the humic substances do not show a signal in negative ion mobility spectrum, the quantitative determination of Acesulfame is considerably affected. Even comparative low concentrations of DOM ( $10 \text{ ng } \mu\text{L}^{-1}$ ) reduce the signal intensity of Acesulfame by 65%. Higher DOM concentrations lead to a further decrease. It is notable that these concentrations are quite low related to the natural occurrence of DOM in water samples. Related to 300 mL water sample (which are typically used in our procedure) and the complete enrichment of DOM in the eluate, these DOM concentrations correspond up to  $0.35 \text{ mg L}^{-1}$  in water samples (values in brackets). These concentrations are much

lower in comparison with the typical occurrence of DOM in natural water samples. Consequently, DOM has to be eliminated as much as possible prior ESI-IMS analysis.

### ***3.4. Matrix effects using paper based MIP disks and ESI-IMS: Interfering trace organic compounds***

The MIP material has a high efficiency to extract Acesulfame but has also a certain cross selectivity towards substances with sulfonyl functionality and amino groups. Do co-extracted substances interfere with the determination of Acesulfame? This question was tackled with the further experiment. For evaluation of selectivity features of our MIPs, the filter paper was loaded with 300 mL water sample containing Acesulfame-K, Bentazon, Saccharin, Ibuprofen sodium salt, Naproxen sodium salt, Atrazine and Caffeine (where the concentration of each solute was  $3.3 \mu\text{g L}^{-1}$ ). In this case, the measurements were done with HPLC-MS-MS. According to our common procedure, the loaded filter paper was dried completely and washed with 10 mL dichloromethane, dried again and then washed with 10 mL methanol. The obtained results (Fig. S3 of the supplementary material) show the selectivity enhancement of filter paper applied for water sample. Filter paper embedded with imprinted polymer sorbents shows the highest affinity towards negatively-charged Acesulfame with a recovery of 65%. Caffeine and Atrazine were removed completely. Two structural analogues, Bentazon and Saccharin which have negatively-charged sulfonamide group at environmental pH values, were extracted with recoveries lower than 24%. Naproxen and Ibuprofen with respective recoveries of 7 % and 3 % did not indicate any interference with the Acesulfame response. This selectivity generally permits the determination of Acesulfame in nearly all natural water samples with ESI-IMS.

### ***3.5. Matrix effects using paper based MIP disks and ESI-IMS: Dissolved organic matter***

Fig. S4 of the supplementary material shows the influence of DOM content on the quantitative results for Acesulfame using our selective extraction procedure with MIP loaded paper filters. Four different water samples containing Acesulfame and humic acid sodium salt were prepared. The volumes of the water samples were 300 mL and the concentrations of Acesulfame were kept constant at  $5.8 \mu\text{g L}^{-1}$ . The concentrations of humic acids were increased from 0 to 2, 4 and  $6 \text{ mg L}^{-1}$ . The peak intensities of Acesulfame are not affected by DOM concentrations up to  $6 \text{ mg L}^{-1}$ . Additional measurements of the spectral absorption coefficient (SAC) at 254 nm have shown that our sample preparation procedure reduces the concentration of DOM to < 3% related to the original concentration. Between 45 and 60% of DOM goes through the filter paper during the extraction, approximately 4-7% were removed during the first washing step with dichloromethane and between 35 and 45% during the second washing step with methanol. Less than 3% were found in the eluate. Related to an initial concentration of  $6 \text{ mg L}^{-1}$ , the eluate contains DOM in concentration less than 5

ng  $\mu\text{L}^{-1}$ . The influence of DOM can be neglected for water samples with average DOM content using our paper based MIP disks.

### **3.6. Method validation and real samples**

The objective of validation of our analytical procedure was to demonstrate that it was suitable for its intended purpose. This included determining the limit of detection (LOD), limit of quantification (LOQ), relative standard deviations (RSD) and reproducibility of the procedure. The optimized parameters for ion mobility measurements permit the sensitive determination of Acesulfame. Without sample preparation,  $93 \mu\text{g L}^{-1}$  was calculated as LOD and  $287 \mu\text{g L}^{-1}$  as LOQ for ion mobility measurements. Standard solutions were prepared within a concentration range of 0.12 and  $31 \mu\text{g L}^{-1}$  and used for the validation of the extraction of Acesulfame from water samples using our sample preparation procedure. These samples were then analyzed using ESI-IMS. The calibration curve could be described with the function ( $y=0.0001x^3-0.012x^2+0.3998x+0.0406$ ) with the coefficient of determination  $R^2=0.9982$ . The LOD for samples analyzed with IMS after preparation using the presented procedure was  $0.19 \mu\text{g L}^{-1}$  and the LOQ was  $0.63 \mu\text{g L}^{-1}$ . These data were calculated according to the Eurachem Guide procedures. The RSDs at different concentrations were between 0.49 and 9.53%.

In order to validate our sampling and extraction procedure, we compared three different analytical approaches for the determination of Acesulfame in samples from a river. A standard procedure using commercial styrene-divinylbenzene (SDB) extraction column containing 200 mg of sorbent was used to compare the selectivity levels of the developed MIP-embedded filter paper. The SPE procedure commonly used for monitoring polar to semi-polar pollutants in water samples was carried out according to [47]. The eluates of the presented procedure were analyzed with HPLC-ESI-MS-MS and ESI-IMS. The samples were taken from the river White Elster (Leipzig, Germany) at locations upstream and downstream of the effluent of the central municipal waste water treatment plant (WWTP, approximately 500,000 population equivalents). The results are summarized in Fig. 6. Due to the low removal efficiency in conventional WWTPs, the concentration of Acesulfame increases downstream the wastewater discharge. Further dilution along the flow path decreases the concentrations of Acesulfame to a comparable level before wastewater input. A very good agreement between the quantitative results for Acesulfame was observed. The SPE (SDB)-MS procedure provided slightly lower concentrations for the samples after the influent of WWTP where the samples are loaded with a complex matrix. The measurements with IMS and MS after the extraction with MIP loaded paper filters provided comparable results. It is notable that the presented ESI-IMS procedure with paper filters is the simplest and fastest method. The paper filters can be loaded in the field and can be used for transportation to the lab instead to transport the water

bottles. We investigated the long-term stability over 4 days without loss of signal intensity for Acesulfame. The measurement with ESI-IMS requires few minutes with a less complex instrumentation.

## 4. Conclusions

We developed a simple and easy-to-handle extraction procedure which requires little equipment for the determination of trace organic compounds in water samples. No transportation of water samples is required. MIPs for the artificial sweetener Acesulfame-K were synthesized. It is an accepted municipal wastewater indicator. The MIPs were embedded in paper filters which can be loaded in the field. The analysis was performed using ESI-IMS with a modified and optimized set-up. It is characterized by a lower complexity of analytical instrument in comparison with mass spectrometry and can be configured as transportable unit. The quantitative results of our method are comparable to those obtained with commonly used standard procedures in the lab. Our method is compatible with any substance where MIPs are available and which is detectable with ESI-IMS. With further advances in ESI-IMS instrumentation like miniaturization, the feasibility for field applications will be improved and the whole protocol can become a mobile, sensor-like instrumentation, fast and robust for on-site monitoring.

## Acknowledgement

The authors gratefully acknowledge the technical support of mechanical workshop of the UFZ (Peter Portius, Manuel Kositzke, Daniel Karmowski, Mathias Wilde) in producing the parts of ion mobility spectrometer. Furthermore, we cordially thank our native speaker, Malcolm Cämmerer, for proofreading the manuscript.

## References

- [1] V. Leendert, H. Van Langenhove, K. Demeestere, Trends in liquid chromatography coupled to high-resolution mass spectrometry for multi-residue analysis of organic micropollutants in aquatic environments, *TrAC Trends in Analytical Chemistry* 67 (2015) 192-208.
- [2] S.D. Richardson, S.Y. Kimura, Water Analysis: Emerging Contaminants and Current Issues, *Anal Chem* 88(1) (2016) 546-82.
- [3] E.L. Schymanski, H.P. Singer, J. Slobodnik, I.M. Ipolyi, P. Oswald, M. Krauss, T. Schulze, P. Haglund, T. Letzel, S. Grosse, N.S. Thomaidis, A. Bletsou, C. Zwiener, M. Ibáñez, T. Portolés, R. de Boer, M.J. Reid, M. Onghena, U. Kunkel, W. Schulz, A. Guillon, N. Noyon, G. Leroy, P. Bados, S. Bogialli, D. Stipanicev, P. Rostkowski, J. Hollender, Non-target screening with high-resolution mass spectrometry: critical review using a collaborative trial on water analysis, *Anal Bioanal Chem* 407(21) (2015) 6237-6255.
- [4] A. Gałuszka, Z.M. Migaszewski, J. Namieśnik, Moving your laboratories to the field – Advantages and limitations of the use of field portable instruments in environmental sample analysis, *Environmental Research* 140 (2015) 593-603.

- [5] R.E. Bain, S.W. Gundry, J.A. Wright, H. Yang, S. Pedley, J.K. Bartram, Accounting for water quality in monitoring access to safe drinking-water as part of the millennium development goals: lessons from five countries, *Bulletin of the World Health Organization* 90 (2012) 228-235.
- [6] V.K. Gupta, M.L. Yola, T. Eren, N. Atar, Selective QCM sensor based on atrazine imprinted polymer: Its application to wastewater sample, *Sensors and Actuators B: Chemical* 218 (2015) 215-221.
- [7] S.D. Richardson, S.Y. Kimura, Water Analysis: Emerging Contaminants and Current Issues, *Anal Chem* 88(1) (2016) 546-582.
- [8] H. Borsdorf, G.A. Eiceman, Ion mobility spectrometry: principles and applications, *Appl Spectrosc Rev* 41(4) (2006) 323-375.
- [9] D. Wittmer, B.K. Luckenbill, H.H. Hill, Y.H. Chen, Electrospray-Ionization Ion Mobility Spectrometry, *Anal Chem* 66(14) (1994) 2348-2355.
- [10] Y.H. Chen, H.H. Hill, D.P. Wittmer, Thermal effects on electrospray ionization ion mobility spectrometry, *Int J Mass Spectrom* 154(1-2) (1996) 1-13.
- [11] C.B. Shumate, H.H. Hill, Coronaspray Nebulization and Ionization of Liquid Samples for Ion Mobility Spectrometry, *Anal Chem* 61(6) (1989) 601-606.
- [12] T. Khayamian, M.T. Jafari, Design for electrospray ionization-ion mobility spectrometry, *Anal Chem* 79(8) (2007) 3199-3205.
- [13] M.T. Jafari, Improved design for high resolution electrospray ionization ion mobility spectrometry, *Talanta* 77(5) (2009) 1632-1639.
- [14] C.J. Bramwell, M.L. Colgrave, C.S. Creaser, R. Dennis, Development and evaluation of a nano-electrospray ionisation source for atmospheric pressure ion mobility spectrometry, *Analyst* 127(11) (2002) 1467-1470.
- [15] M.L. Colgrave, C.J. Bramwell, C.S. Creaser, Nanoelectrospray ion mobility spectrometry and ion trap mass spectrometry studies of the non-covalent complexes of amino acids and peptides with polyethers, *Int J Mass Spectrom* 229(3) (2003) 209-216.
- [16] A.B. Kanu, B.S. Kumar, H.H. Hill, Evaluation of micro- versus nano-electrospray ionization for ambient pressure ion mobility spectrometry, *Int J Ion Mobility Spectrom* 15(1) (2011) 9-20.
- [17] X. Tang, J.E. Bruce, H.H. Hill, Jr., Characterizing electrospray ionization using atmospheric pressure ion mobility spectrometry, *Anal Chem* 78(22) (2006) 7751-60.
- [18] L.W. Beegle, I. Kanik, L. Matz, H.H. Hill, Electrospray ionization nigh-resolution ion mobility spectrometry for the detection of organic compounds, 1. Amino acids, *Anal Chem* 73(13) (2001) 3028-3034.
- [19] T. Reinecke, A.T. Kirk, A. Ahrens, C.R. Raddatz, C. Thoben, S. Zimmermann, A compact high resolution electrospray ionization ion mobility spectrometer, *Talanta* 150 (2016) 1-6.
- [20] G.R. Asbury, H.H. Hill, Negative Ion Electrospray Ion Mobility Spectrometry, *Int J Ion Mobility Spectrom* 2(1) (1998) 1-8.
- [21] G. Wulff, Molecular Imprinting in Cross-Linked Materials with the Aid of Molecular Templates - a Way Towards Artificial Antibodies, *Angewandte Chemie-International Edition in English* 34(17) (1995) 1812-1832.
- [22] Zarejousheghani M, Fiedler P, Möder M, B. H, Selective mixed-bed solid phase extraction of atrazine herbicide from environmental water samples using molecularly imprinted polymer, *Talanta* 129 (2014) 132-138.
- [23] M. Zarejousheghani, M. Moder, H. Borsdorf, A new strategy for synthesis of an in-tube molecularly imprinted polymer-solid phase microextraction device: Selective off-line extraction of 4-nitrophenol as an example of priority pollutants from environmental water samples, *Anal Chim Acta* 798 (2013) 48-55.
- [24] A.L. Capriotti, C. Cavaliere, P. Foglia, R. Samperi, S. Stampachiachiere, S. Ventura, A. Lagana, Recent advances and developments in matrix solid-phase dispersion, *Trac-Trend Anal Chem* 71 (2015) 186-193.
- [25] A. Prieto, A. Vallejo, O. Zuloaga, A. Paschke, B. Sellergen, E. Schillinger, S. Schrader, M. Moder, Selective determination of estrogenic compounds in water by microextraction by packed sorbents

and a molecularly imprinted polymer coupled with large volume injection-in-port-derivatization gas chromatography-mass spectrometry, *Anal Chim Acta* 703(1) (2011) 41-51.

[26] M. Zarejousheghani, S. Schrader, M. Möder, M. Schmidt, H. Borsdorf, A new strategy for accelerated extraction of target compounds using molecularly imprinted polymer particles embedded in a paper-based disk, *Journal of Molecular Recognition* 31(3) (2018) e2629-n/a.

[27] R.E. Ranney, J.A. Oppermann, E. Muldoon, F.G. McMahon, Comparative metabolism of aspartame in experimental animals and humans, *Journal of Toxicology and Environmental Health* 2(2) (1976) 441-451.

[28] B. Subedi, K. Kannan, Fate of Artificial Sweeteners in Wastewater Treatment Plants in New York State, U.S.A, *Environ Sci Technol* 48(23) (2014) 13668-13674.

[29] Z.Y. Sang, Y.A. Jiang, Y.K. Tsoi, K.S.Y. Leung, Evaluating the environmental impact of artificial sweeteners: A study of their distributions, photodegradation and toxicities, *Water Research* 52 (2014) 260-274.

[30] G.-W. von Rymon Lipinski, The new intense sweetener Acesulfame K, *Food Chem* 16(3) (1985) 259-269.

[31] I.J. Buerge, H.R. Buser, M. Kahle, M.D. Muller, T. Poiger, Ubiquitous Occurrence of the Artificial Sweetener Acesulfame in the Aquatic Environment: An Ideal Chemical Marker of Domestic Wastewater in Groundwater, *Environ Sci Technol* 43(12) (2009) 4381-4385.

[32] Z.W. Gan, H.W. Sun, B.T. Feng, R.N. Wang, Y.W. Zhang, Occurrence of seven artificial sweeteners in the aquatic environment and precipitation of Tianjin, China, *Water Research* 47(14) (2013) 4928-4937.

[33] J.W. Roy, D.R. Van Stempvoort, G. Bickerton, Artificial sweeteners as potential tracers of municipal landfill leachate, *Environmental Pollution* 184 (2014) 89-93.

[34] I.J. Buerge, T. Poiger, Acesulfame: From Sugar Substitute to Wastewater Marker, *Chimia* 65(3) (2011) 176.

[35] M.G. Kokotou, N.S. Thomaidis, Determination of eight artificial sweeteners in wastewater by hydrophilic interaction liquid chromatography-tandem mass spectrometry, *Anal Methods-Uk* 5(16) (2013) 3825-3833.

[36] H.S. Lim, S.K. Park, I.S. Kwak, H.I. Kim, J.H. Sung, S.J. Jang, M.Y. Byun, S.H. Kim, HPLC-MS/MS analysis of 9 artificial sweeteners in imported foods, *Food Sci Biotechnol* 22(1) (2013) 233-240.

[37] Q.C. Chen, J. Wang, Simultaneous determination of artificial sweeteners, preservatives, caffeine, theobromine and theophylline in food and pharmaceutical preparations by ion chromatography, *J Chrom A* 937(1-2) (2001) 57-64.

[38] V.N.O. Fernandes, L.B. Fernandes, J.P. Vasconcellos, A.V. Jager, F.G. Tonin, M.A.L. de Oliveira, Simultaneous analysis of aspartame, cyclamate, saccharin and acesulfame-K by CZE under UV detection, *Anal Methods-Uk* 5(6) (2013) 1524-1532.

[39] C.J. Musto, S.H. Lim, K.S. Suslick, Colorimetric Detection and Identification of Natural and Artificial Sweeteners, *Anal Chem* 81(15) (2009) 6526-6533.

[40] M. Zarejousheghani, S. Schrader, M. Möder, M. Schmidt, H. Borsdorf, A new strategy for accelerated extraction of target compounds using molecularly imprinted polymer particles embedded in a paper-based disk, *Journal of Molecular Recognition* (2017) e2629-n/a.

[41] M. Zarejousheghani, S. Schrader, M. Möder, P. Lorenz, H. Borsdorf, Ion-exchange molecularly imprinted polymer for the extraction of negatively charged acesulfame from wastewater samples, *J Chrom A* 1411 (2015) 23-33.

[42] T. Henriksen, R.K. Juhler, B. Svensmark, N.B. Cech, The relative influences of acidity and polarity on responsiveness of small organic molecules to analysis with negative ion electrospray ionization mass spectrometry (ESI-MS), *J Am Soc Mass Spectr* 16(4) (2005) 446-455.

[43] A. Krueve, K. Kaupmees, J. Liigand, I. Leito, Negative electrospray ionization via deprotonation: predicting the ionization efficiency, *Anal Chem* 86(10) (2014) 4822-30.

[44] <https://comptox.epa.gov/dashboard/>

[45] A. Krueve, Influence of mobile phase, source parameters and source type on electrospray ionization efficiency in negative ion mode, *J Mass Spectrom* 51(8) (2016) 596-601.

[46] A. Krüve, K. Kaupmees, Predicting ESI/MS Signal Change for Anions in Different Solvents, *Anal Chem* 89(9) (2017) 5079-5086.

[47] M. Scheurer, H.J. Brauch, F.T. Lange, Analysis and occurrence of seven artificial sweeteners in German waste water and surface water and in soil aquifer treatment (SAT), *Anal Bioanal Chem* 394(6) (2009) 1585-1594.

## Figure captions

**Fig. 1.** Influence of solvent composition on signal intensity (measurements with  $10 \text{ ng } \mu\text{L}^{-1}$  per substance)

**Fig. 2.** Influence of experimental conditions on signal intensity (A: inner diameter of emitter tip, B: solvent flow rate through the emitter, C: temperature of ion mobility spectrometer, D: gas flow through the ion mobility spectrometer, the concentrations in B, C, D were approximately  $10 \text{ ng } \mu\text{L}^{-1}$  per substance and methanol was used as solvent)

**Fig. 3.** Influence of experimental conditions on drift times (A: temperature of ion mobility spectrometer and B: gas flow through the ion mobility spectrometer with concentrations of approximately  $10 \text{ ng } \mu\text{L}^{-1}$  per substance)

**Fig. 4.** Dependence of signal intensity of Acesulfame on the presence of matrix compounds (A: Signal intensity of Acesulfame as pure substance and in mixture with Saccharin and/or Bentazon; B: Dependence of the signal intensity of Acesulfame (ACE) on the concentration of Bentazon (BENT), the concentration of Acesulfame was kept constant with increasing concentrations of Bentazon)

**Fig. 5.** Influence of dissolved organic matter on the determination of Acesulfame (DOM was dissolved in methanol and injected into the ion mobility spectrometer. The concentrations in brackets were counted back to 300 mL water sample with a recovery of 100%)

**Fig. 6.** Concentration of Acesulfame along a river at locations upstream and downstream of the effluent of a waste water treatment plant (WWTP)

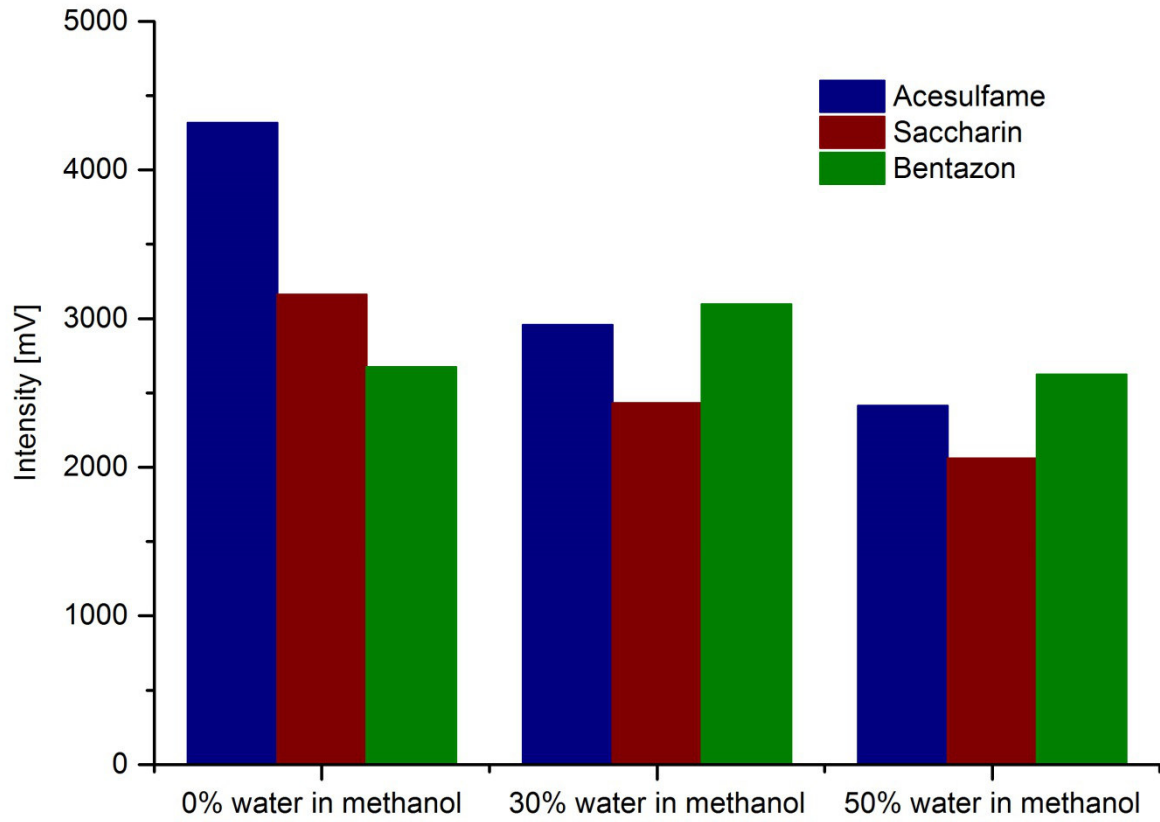


**Fig. 1.** Influence of solvent composition on signal intensity (measurements with  $10 \text{ ng } \mu\text{L}^{-1}$  per substance)

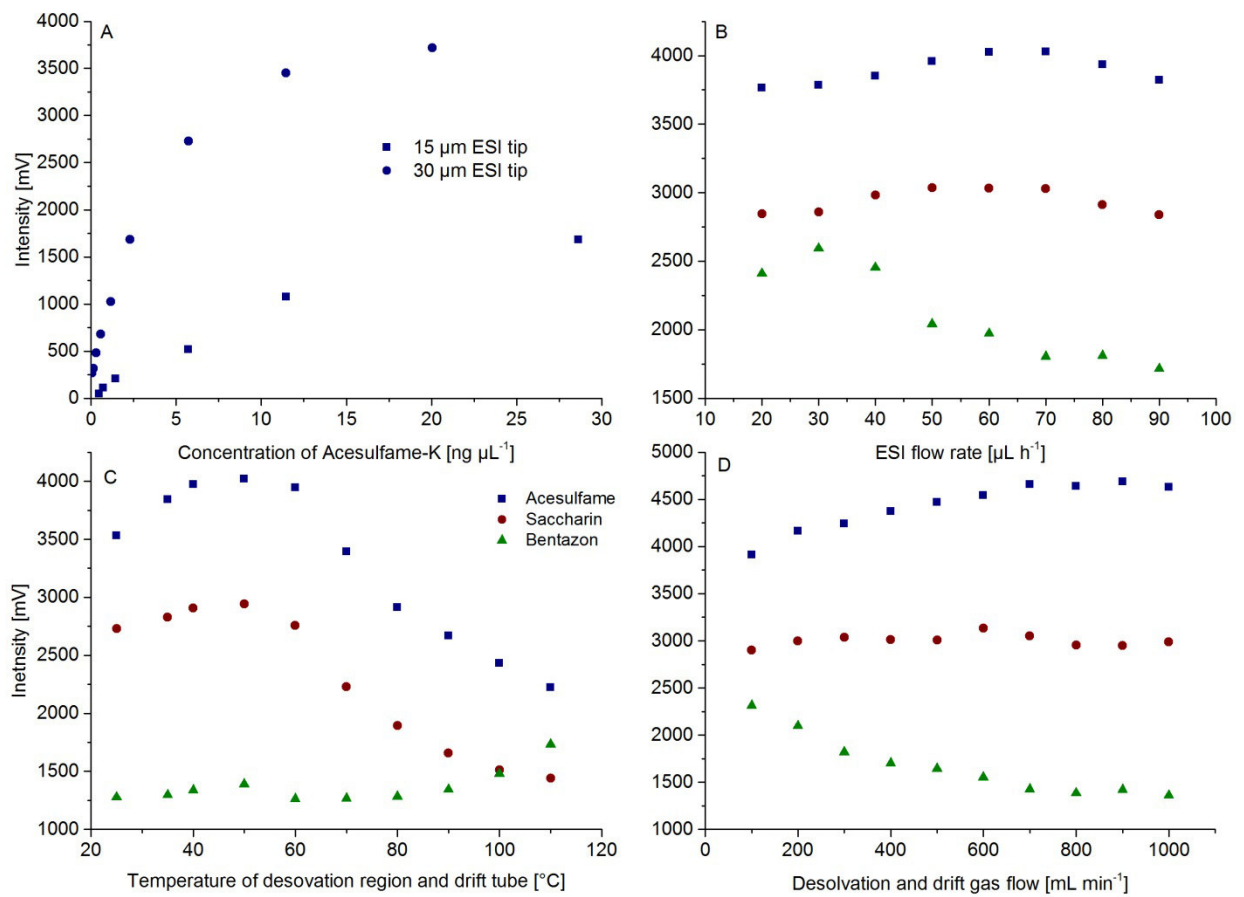


**Fig. 2.** Influence of experimental conditions on signal intensity (A: inner diameter of emitter tip, B: solvent flow rate through the emitter, C: temperature of ion mobility spectrometer, D: gas flow through the ion mobility spectrometer, the concentrations in B, C, D were approximately  $10 \text{ ng } \mu\text{L}^{-1}$  per substance and methanol was used as solvent)

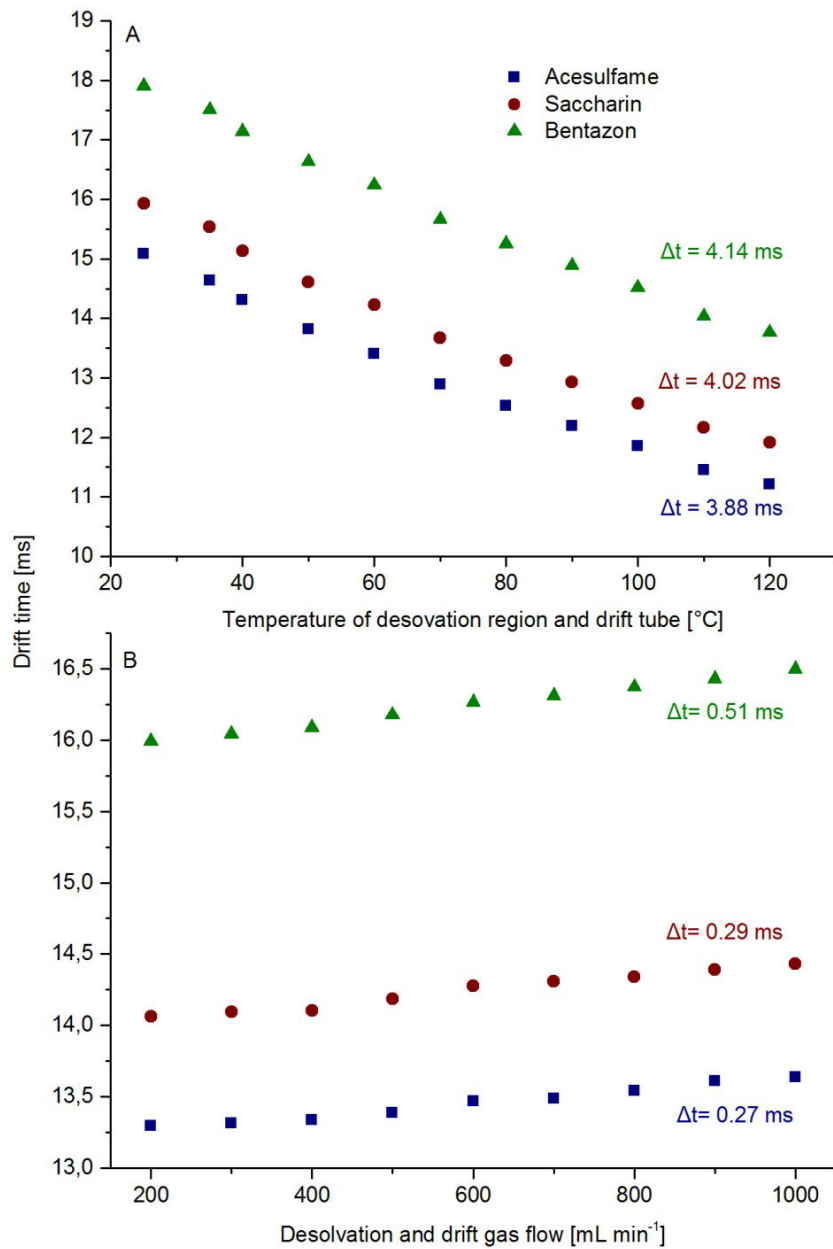


**Fig. 3.** Influence of experimental conditions on drift times (A: temperature of ion mobility spectrometer and B: gas flow through the ion mobility spectrometer with concentrations of approximately 10 ng  $\mu\text{L}^{-1}$  per substance)

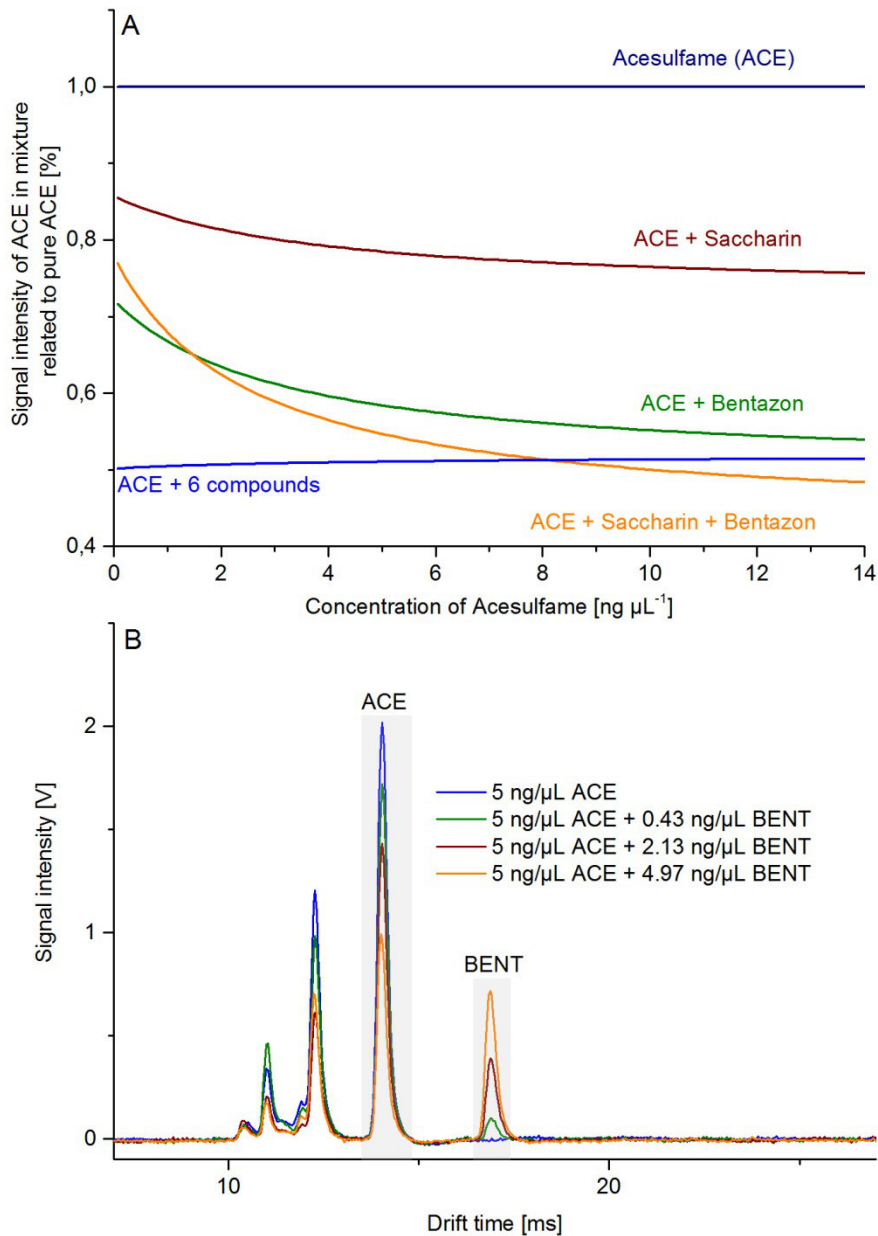


**Fig. 4.** Dependence of signal intensity of Acesulfame on the presence of matrix compounds (A: Signal intensity of Acesulfame as pure substance and in mixture with Saccharin and/or Bentazon; B: Dependence of the signal intensity of Acesulfame (ACE) on the concentration of Bentazon (BENT), the concentration of Acesulfame was kept constant with increasing concentrations of Bentazon)

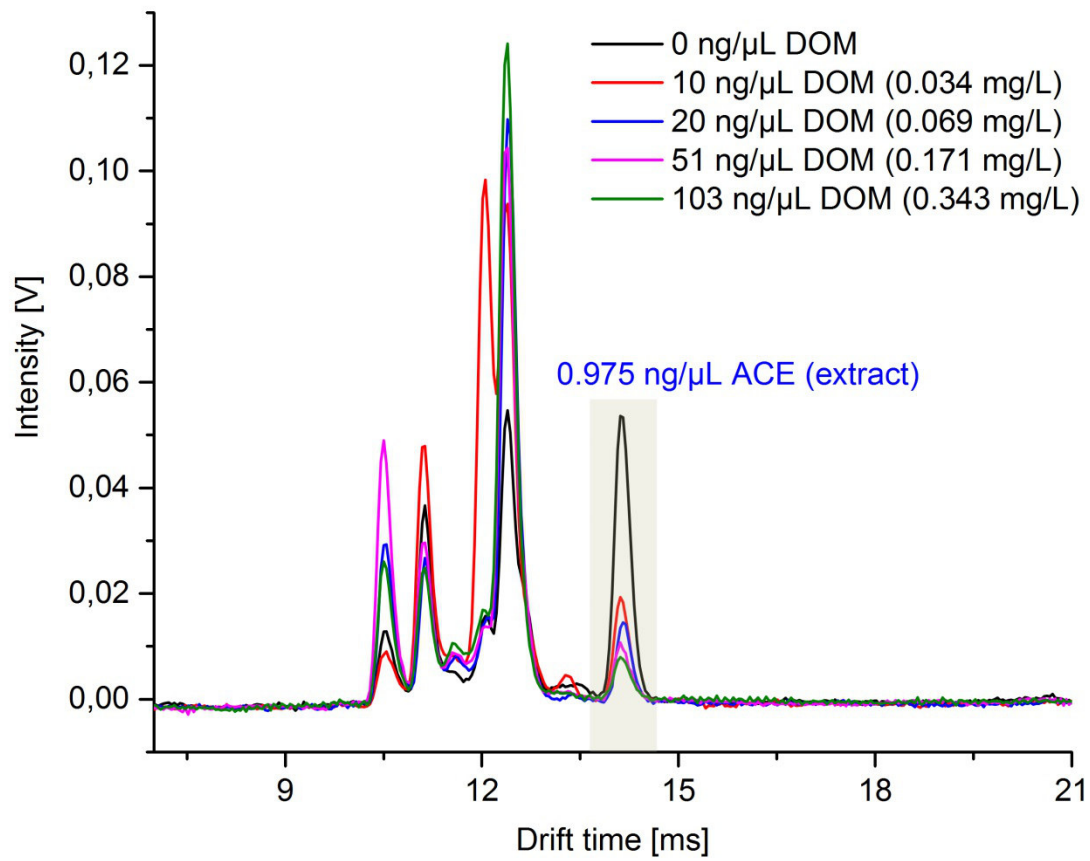


**Fig. 5.** Influence of dissolved organic matter on the determination of Acesulfame (DOM was dissolved in methanol and injected into the ion mobility spectrometer. The concentrations in brackets were counted back to 300 mL water sample with a recovery of 100%)

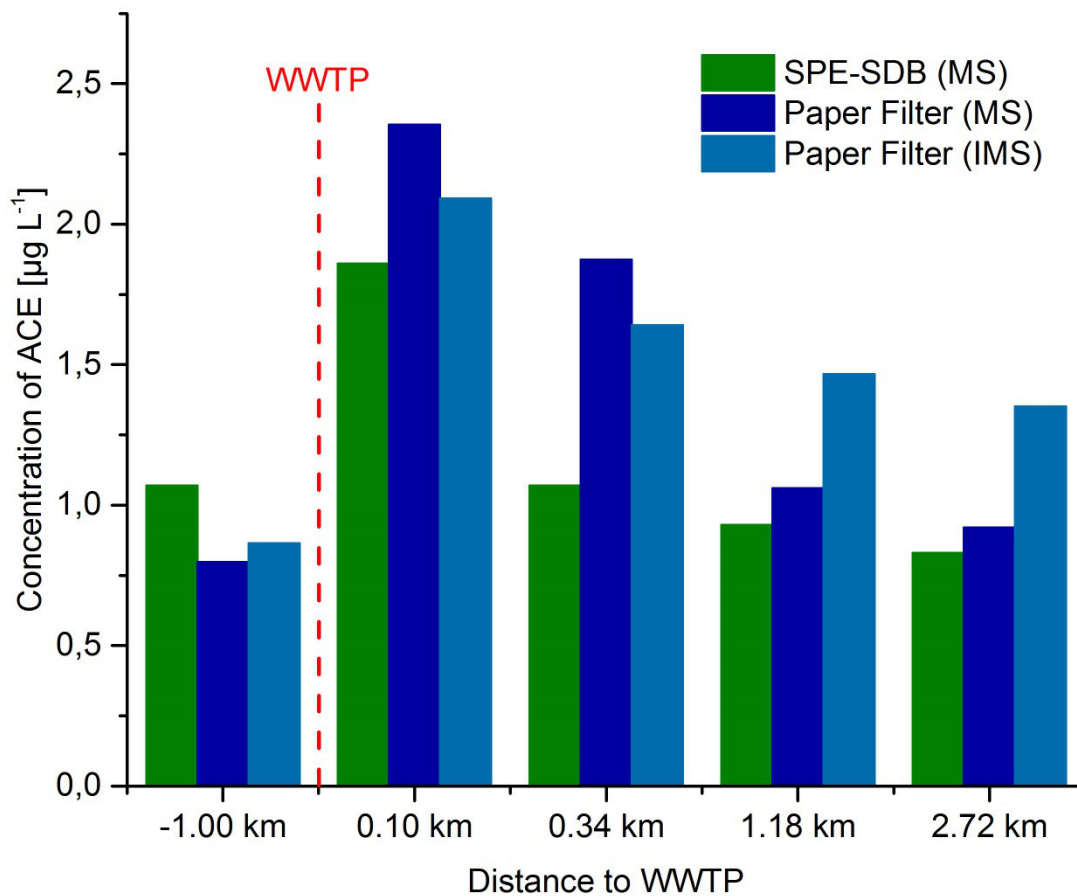


**Fig. 6.** Concentration of Acesulfame along a river at locations upstream and downstream of the effluent of a waste water treatment plant (WWTP)